

Do You Need a Hand? – a Bimanual Robotic Dressing Assistance Scheme

Jihong Zhu^{1,3}, Michael Gienger², Giovanni Franzese³, and Jens Kober³

Abstract—Developing physically assistive robots capable of dressing assistance has the potential to significantly improve the lives of the elderly and disabled population. However, most robotics dressing strategies considered a single robot only, which greatly limited the performance of the dressing assistance. In fact, healthcare professionals perform the task bimanually. Inspired by them, we propose a bimanual cooperative scheme for robotic dressing assistance. In the scheme, an interactive robot joins hands with the human thus supporting/guiding the human in the dressing process, while the dressing robot performs the dressing task. We identify a key feature that affects the dressing action and propose an optimal strategy for the interactive robot using the feature. A dressing coordinate based on the posture of the arm is defined to better encode the dressing policy. We validate the interactive dressing scheme with extensive experiments and also an ablation study. The experiment video is available on <https://sites.google.com/view/bimanualassistdressing/home>

I. INTRODUCTION

The shortage of caregivers is a pressing challenge worldwide due to a decrease in birth rates combined with an increase in life expectancy: according to the WHO, by 2030, 1 in 6 people in the world will be aged 60 years or over. By 2050, the world’s population of people aged 60 years and older will double [1]. Assistive robots capable of physically aiding humans are promising to tackle this challenge. Among various tasks that the caregiver performs on a daily basis, the dressing was reported to be the greatest burden while the least automated [2]. In this paper, we tackle the problem of dressing a human arm with a bimanual robot setup.

Robot-assisted dressing is challenging as it involves direct physical interaction with flexible clothes and humans. More specifically, it differs from a conventional human-robot interaction task such as co-manipulation or co-carrying [3]–[5] where the object allows immediate force propagation. In the dressing assistance, the object i.e. the cloth, is soft and deformable, thus, the interaction force is hard to obtain. Due to the absence of direct force feedback and heavy occlusion during dressing, arm movement estimation during dressing is also difficult.

One common assumption to simplify the task is to consider static arm posture during dressing. Then the main challenge becomes adapting the dressing policy to different static postures. Learning from demonstrations (LfD) is often used in obtaining a generalized policy [6]–[8].

¹J. Zhu is with University of York, the UK jihong.zhu@york.ac.uk

²M. Gienger is with Honda Research Institute Europe, Germany michael.gienger@honda-ri.de

³J. Zhu, G. Franzese, and J. Kober are with Cognitive Robotics, 3mE, Delft University of Technology, Netherlands {J.Zhu-3,G.Franzese,J.Kober}@tudelft.nl

However, a static arm posture is a very strong assumption. To make the proposed scheme work in practice, we need to consider dynamic poses during dressing. Since the task largely depends on postures, arm movement estimation is crucial.

Computer vision is a popular way to track arm postures. It is also used in the early work in assistive dressing [9] for tracking upper limb movement. However, the inevitable occlusions during dressing render most of the existing vision-based human posture tracking algorithms fail [10], [11]. Additional sensory modules, such as proximity sensors may be employed for posture estimation [12].

To overcome the difficulties faced with conventional assistive dressing strategies, we draw inspiration from human-to-human dressing assistance from healthcare professionals¹. Our proposed framework resembles the method adapted by health professionals. It requires two robots to perform the dressing assistance task. An interactive robot \mathcal{I} that reaches out for holding hands with the human, then supports/guides the human to facilitate the dressing process. The dressing robot \mathcal{D} performs the main task, dressing. Hand holding not only makes the dressing task easier to execute by supporting/guiding the human arm movement but also results in the tracking of the arm posture with proprioceptive sensors only.

The main contribution of the paper is the proposal of a bimanual dressing assistance framework, which is unprecedented in previous robotics research. In the framework, instead of considering interaction forces during dressing which is often hard to obtain in practice [13], we offer a novel perspective by analysing dressing geometrically. Benefiting from this new insight, we identify a key feature in the human posture that affects dressing policy. The feature is then used for designing an optimal stretch policy for the interactive robot. For the dressing, in contrast to encoding the movement in Cartesian space, we define a task coordinate system for flexible policy encoding from demonstrations.

The paper is organized as follows: In Sect. II we survey the related work in three subcategories, namely: robotic dressing assistance, bimanual manipulation, and arm poster estimation. Sect. III provides an overview of the overall framework. Sect. IV introduces the feature that affects the dressing strategy and then designs an optimal strategy for the interactive robot \mathcal{I} based on the feature. With the information on the hand position given by the \mathcal{I} , we can solve the arm posture with proprioceptive sensors only. Later in Sect. V, we propose a dressing coordinate dependent on arm postures, then learn the dressing policy from expert demonstrations in the dressing

¹<https://youtu.be/Wn1OEfQt0ow?t=93>

coordinate. The overall framework is validated with robotic experiments in Sect. VI. Finally in Sect. VII, we conclude.

II. RELATED WORK

A. Robotic Dressing Assistance

Robotic dressing assistance is a recurrent topic that broadly covers dressing tops (t-shirt, jacket, etc.) [14], trousers [15] and even shoes [16], [17]. Since in this paper, our focus is dressing the upper body, we review recent advances, particularly in this area.

Dressing assistance is a skill mastered by humans. Therefore, LfD-based approaches are popular in obtaining motor skills in dressing. Pignat and Calinon learned a hidden semi-Markov model [6] from human demonstrations to encode the dressing skills. The authors of [7] implemented an incremental learning of Task-Parameterized Gaussian Mixture Models (TP-GMM) that allows generalization of the dressing task. More recently, [8] proposed a method to reduce the number of demonstrations needed for training the TP-GMM to encode a dressing policy in different static postures.

Recent research also explores the interaction between a robot and a human in the dressing process with reinforcement learning in a simulation environment [18], [19]. The authors of [20] learned an outcome classifier for dressing tasks with simulated haptic data. Instead of relying on simulations, data collected in the real dressing scenarios suggests that the interaction force between the cloth and the human allows for predicting dressing outcomes with high accuracy [21]. Later, Erickson et al. [22] conducted an investigation with physics-based simulation suggesting that the interaction force can be recovered with only end-effector measurements.

Further research in this area is concerned with cloth state modeling [23], safe motion planning [24], [25], grasping point selection [26] and novel gripper design for dressing assistance [27].

In the above-mentioned research, the dressing tasks were mostly conducted with a single manipulator. The only papers considering bimanual dressing are [14], [19]. However, they consider the bimanual in a completely different setup where each robot is dressing one human arm respectively. Therefore, they adopt the *one-robot-to-one-arm* setup just like the rest of the papers. In our proposal, we have instead a *two-robot-to-one-arm* setup, where a robot is guiding humans to facilitate the dressing task of the other robot.

B. Bimanual Manipulation

In the proposed framework, we adopt implicit master-slave coordination between the interactive and the dressing robots. The dressing policy is dependent on the human arm posture which is controlled by the interactive robot from the applied guidance force on the human hand. Such task setup is referred to as asymmetrical bimanual manipulation in the bimanual taxonomy literature [28].

The asymmetrical bi-manual task that was investigated in the previous work includes: vegetable peeling [29], cloth manipulation [30], assembly [31] and cooking [32]. These

tasks usually do not require interaction with a human as in the dressing assistance.

More relevant bimanual assistive tasks: Xu et al. designed an autonomous wheelchair with two robots to assist humans in daily tasks [33]. Connan et al. employed a humanoid robot to perform tasks such as removing the lid, unscrewing a bottle, and pouring water [34]. Edsinger and Kemp discussed three key themes in bimanual manipulation design in assistive tasks: cooperative manipulation, tasks relevant features, let the body do the thinking and analysed them in different assistive scenarios [35]. These key themes remain very relevant to us in designing the framework for this paper.

To date, robotics dressing assistance (specifically dressing clothes) has never been considered a bimanual task that requires both robots. However, as we argued in Sect. I, the additional robot can provide support and guidance to the arm being dressed, which makes the dressing easier and more comfortable. As the scheme is employed by caregiving professionals, humans might feel more contented dressing in such a composition. By adopting the bimanual setup in dressing, our work is the first of its kind and represents a paradigm shift in thinking of the dressing assistance task.

C. Arm Posture Estimation

The dressing policy is highly dependent on human arm posture. As the guidance force at hand will change the human arm posture in our framework, a robust arm posture tracking/estimation is required for dressing policy generation.

Due to heavy occlusion during dressing, the task is particularly challenging for popular vision-based deep learning posture tracking algorithm [36]–[39].

Human modeling is employed for tracking the human posture under occlusions. A preliminary study in dressing assistance considers human modeling combined with visual tracking in personalized dressing: the authors of [9] adopted a mixture of Gaussians for modeling, and later a Gaussian process latent variable model (GP-LVM) was employed for posture estimation in [10]. Recently, the author of [11] tackled the occlusion problem by employing a recurrent neural network trained on human-human interaction data to predict the elbow position during dressing. Rather than relying on vision alone, previous works also explored capacitive proximity sensing [12] for posture tracking.

In this paper, we will demonstrate that tracking is made easy by hand-holding. With the hand position always known, arm posture tracking can be formulated as an inverse kinematic problem that has analytical solutions and is solvable in real-time with proprioceptive sensors.

III. FRAMEWORK OVERVIEW

We envision a bimanual dressing assistance system that:

- 1) provides support/guidance to the human arm so as to facilitate dressing,
- 2) tracks the arm posture without additional sensors (vision/force/proximity),
- 3) can be programmed easily without expert knowledge of robotics,

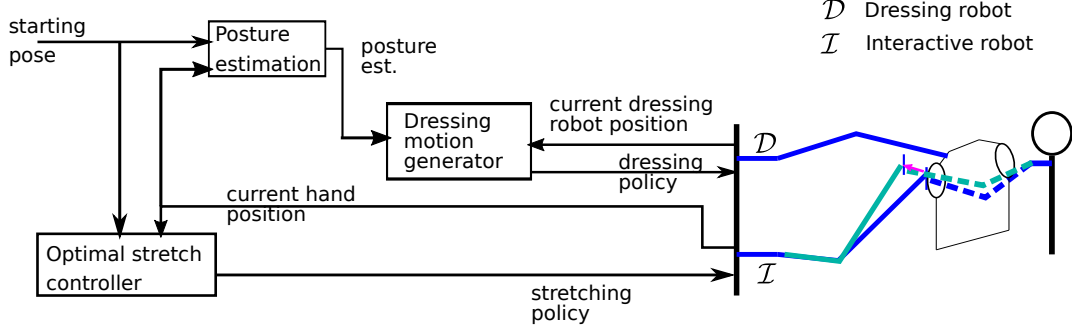


Fig. 1. The schematic diagram of cooperative dressing framework. The framework contains three blocks: a posture estimation, a dressing motion generator, and an optimal stretch controller. The posture estimation takes in an initial posture of the human arm and the current hand position and outputs the estimated current arm posture. The posture is then fed into the dressing motion generator together with the current dressing robot position to derive the next step dressing policy. The optimal stretch controller takes the initial human arm posture and the current hand posture yields the stretching policy for the interactive robotics arm.

4) and flexible to arms of different lengths.

Fig. 1 presents the overall cooperative dressing scheme that fulfills the above goals. The framework contains three parts: an optimal stretch controller, a posture estimation, and a dressing motion generator.

The optimal stretch controller is designed by analysing dressing behaviours under different arm postures to facilitate dressing. The optimal stretch controller takes in the initial human arm posture together with the current hand position and yields the stretching policy for the interactive robot (see Sect. IV-B).

Benefiting from the hand holding, the posture tracking is done by the posture estimation module which takes in the same inputs as the stretch controller and outputs the estimated current arm posture (see Sect. IV-C). It relies solely on proprioceptive sensors.

Using the estimated posture, we define a posture-dependent dressing coordinate and transform the robot movement in the Cartesian coordinate to the dressing coordinate for learning the dressing motion generator from human demonstrations. The dressing can be programmed by non-expert users with kinesthetic teaching. The defined dressing coordinate enables flexible encoding of the dressing strategy to adapt to different arm lengths. Inputs to the dressing motion generator are the estimated posture together with the current dressing robot position. Using the inputs, it generates the next step dressing policy (see Sect. V).

The scheme described above is realized with a bimanual robot setup illustrated in Fig. 2. The dressing robot grips the cloth and executes the dressing policy. The interactive robot is equipped with a SoftHand from qbrobotics that provides human-like hand-holding. It supports and guides the human in the dressing process.

In addition, we employ the following assumptions:

- The starting arm posture is known,
- The shoulder remains static during dressing.

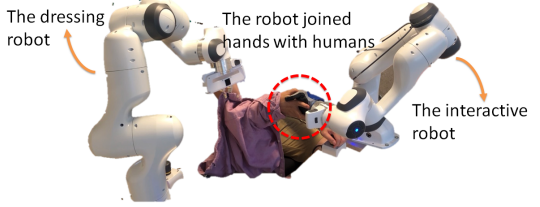


Fig. 2. The bimanual robot setup for the cooperative dressing. We employ two Franka Emika robots. The dressing robot grips the cloth and executes the dressing policy. The interactive robot is equipped with a SoftHand from qbrobotics that provides human-like hand-holding. It guides the human in the dressing process.

IV. INTERACTIVE ROBOT – OPTIMAL STRETCH

In this section, we motivate a key feature in the human arm posture that affects the dressing policy. Based on this feature, we design an optimal stretch controller for the interactive robot. Finally, we present a scheme for the estimation of human arm posture during dressing.

A. The feature affects dressing – elbow angle

The dressing gets complicated around the elbow. If we simplify the forearm and the upper arm as two straight lines, then the discontinuity between these two lines is the linking point (elbow) which connects both lines. The degree of discontinuity can be represented by the elbow angle $\psi \leq \pi$. The angle ψ is a pure geometrical feature that influences the dressing policy.

If we neglect force and only consider geometry, dressing resembles a hotwire game. The cloth can be simplified into a ring that represents the armhole (more formally referred to as the armscye in textile literature), and the arm is the wire that the ring needs to pass through. The goal of dressing is to transport the ring to a position above the shoulder.

However, a major difference that complicates the dressing task is the nature of the ring. In a hotwire game, the ring is rigid. All points on the ring move simultaneously with the

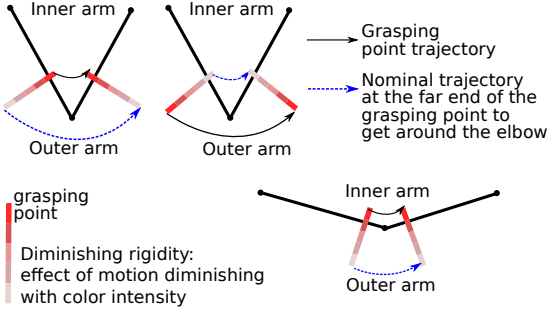


Fig. 3. Illustration of diminishing rigidity on the armscye of the cloth and its influence on the dressing strategy. We consider the arm plane defined by the hand, elbow and shoulder. The arm plane is divided into two parts: the inner arm area with an angle less than π and the outer area with an angle more than π .

grasping/control point on the ring. In dressing, due to the deformation nature of the armscye, we observe the property of diminishing rigidity [40] in the armscye – i.e. that the effect of gripper motion along the armscye diminishes as the distance from the gripper increases. On the bottom left of Fig. 3, we display this effect with color intensity.

In Fig. 3, we define the arm plane: the plane given by shoulder, elbow, and hand positions. The plane is divided by the arm into two parts, inner arm area (angle between the forearm and upper arm less than π) and outer arm area (angle between the forearm and upper arm larger than π). To go past a corner (in dressing case the elbow), we distinguish two different strategies²:

- inner strategy: the projection of the path on the arm plane is within the inner arm area. This strategy offers a shorter path to go around the elbow
- outer strategy: the projection of the path on the arm plane is within the outer arm area. This strategy offers a longer path to go around the elbow.

When ψ is small, taking the inner strategy, the far end of armscye where we have very little control needs to travel much longer to go pass the elbow (See Fig. 3). There is a high possibility it fails and results in the armscye getting stuck. It is more plausible in this case to take the outer strategy, although travels longer in distance, it makes sure that the end with the least control is required to move as little as possible to minimize the chance of getting stuck. When ψ is larger, the distance difference between an inner and outer strategy diminishes and becomes zero when the arm is fully stretched: $\psi = \pi$.

To conclude, elbow angle ψ affects the dressing strategy. When ψ is large, the degree of discontinuity becomes small (the arm resembles a straight line), and we are more likely to take the inner strategy to have a smaller path length. When ψ is small, the degree of discontinuity gets large (the arm is more bend), and we will more likely to take the outer strategy to avoid getting stuck. We will show this effect with

²The trivial case of the shoulder, elbow, and hand is in a line: we cannot define a plane anymore, yet there is also no difference between an inner and outer arm area.

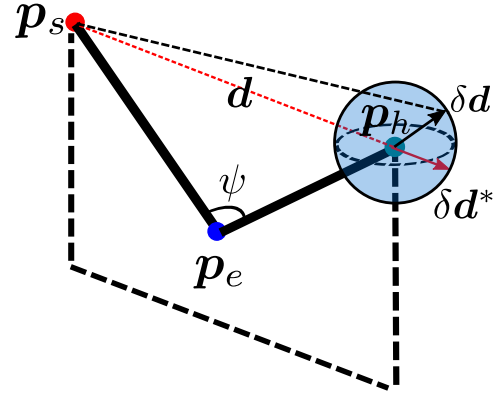


Fig. 4. The optimal direction that maximizes the increase of the elbow angle ψ . The arm posture is given by the shoulder, elbow, and hand joint positions: $\mathbf{P} = \{p_s, p_e, p_h\}$. The optimal direction δd^* is aligned with the direction that connects the hand and the shoulder and marked with a red solid arrow. The triangle inequality theorem is demonstrated with another random direction δd and the resulting shoulder-to-hand distance is marked with a black dash line.

expert demonstration data on different static arm postures (with different elbow angles) in Sect. VI-A.

B. Optimal stretch based on the elbow angle

The outer strategy requires a longer dressing trajectory, and when ψ is small, there is always the risk of getting stuck even taking the outer strategy. Thus, the objective of the interactive robot is to guide the human arm so that ψ increases as much as possible to avoid getting stuck and facilitate dressing.

The interactive robot is holding the human hand. Besides the singular configuration where the arm is fully stretched, the robot is able to guide the hand to move in all directions in 3D which is represented by the blue sphere in Fig. 4. In the figure, the arm posture is given by the shoulder, elbow, and hand joint positions: $\mathbf{P} = \{p_s, p_e, p_h\}$. The movement direction δd that maximizes the increase of the elbow angle, here referred to as δd^* , is aligned with the direction of $\vec{p}_s \vec{p}_h$. Proving the optimal direction is straightforward, since $\psi \propto |\mathbf{d} + \delta \mathbf{d}|$, finding $\delta \mathbf{d}^*$ that maximizes ψ is equivalent to:

$$\delta \mathbf{d}^* = \max_{\delta \mathbf{d}} |\mathbf{p}_s \mathbf{p}_h + \delta \mathbf{d}|, \text{ for } \delta \rightarrow 0, \text{ and } \mathbf{d} \in \text{O}(3)$$

With the triangle inequality theorem, we have:

$$|\mathbf{p}_s \mathbf{p}_h + \delta \mathbf{d}| \leq |\mathbf{p}_s \mathbf{p}_h| + |\delta \mathbf{d}|$$

The maximum value for $|\mathbf{p}_s \mathbf{p}_h + \delta \mathbf{d}|$ is when the equality holds. And it only holds when $\delta \mathbf{d}$ and $\mathbf{p}_s \mathbf{p}_h$ are in the same direction.

Therefore, to increase the elbow angle as much as possible, the guidance force direction from the interactive robot should always be aligned with the direction that connects the hand and the shoulder.

Knowing the optimal direction to move, we further implement the optimal stretch controller with Cartesian impedance control. The end-effector dynamics of a conventional Cartesian impedance controller is [41]:

$$\Lambda \ddot{\mathbf{x}} + \mathbf{D} \dot{\mathbf{x}} + \mathbf{K}(\mathbf{x} - \mathbf{x}_d) = \mathbf{f}_{\text{ext}}^x, \quad (1)$$

where the \mathbf{A} is the Cartesian inertia matrix, \mathbf{K} is a non-diagonal stiffness matrix, and \mathbf{D} is the corresponding critical damping matrix [42]. \mathbf{x}_d is the desired end-effector position. \mathbf{x} , $\dot{\mathbf{x}}$, $\ddot{\mathbf{x}}$ and \mathbf{f}_{ext} are current end-effector position, velocity, acceleration, and external force in the base Cartesian coordinate.

Given a rotation matrix $\mathbf{\Gamma}$ of a local stiffness matrix with respect to the global coordinate, the equivalent stiffness matrix in global coordinates is

$$\mathbf{K}_{\text{global}} = \mathbf{\Gamma}^T \mathbf{K}_{\text{local}} \mathbf{\Gamma} \quad (2)$$

where in our framework, the rotation matrix $\mathbf{\Gamma}$ transforms the x -axis of the global coordinates in the direction of end effector movements that maximizes the increase of the human elbow angle ψ , i.e. $\overrightarrow{p_s p_h}$.

Additionally, we choose

$$\mathbf{K}_{\text{local}} = \begin{bmatrix} k_x & 0 & 0 \\ 0 & 0 & 0 \\ 0 & 0 & 0 \end{bmatrix},$$

in order to have a non-zero stiffness only in the direction of movement and complete compliance in the other two perpendicular directions: such a controller will provide a guiding force in the optimal direction of hand movement that maximizes the increase of the elbow angle ψ . At the same time, the human can disagree and move easily in the plane perpendicular to the force direction.

C. Human arm posture estimation

With the guidance force upon the hand, the human arm posture is changing during dressing. For successfully dressing the human arm, we propose a vision-free estimation of the human arm posture.

Consider two coordinate frames \mathcal{O}^D , \mathcal{O}^I located at the base of each robot respectively. Any point \mathbf{x}^I in \mathcal{O}^I can be transformed into \mathcal{O}^D by:

$$\mathbf{x}^D = \mathbf{R}\mathbf{x}^I + \mathbf{t}. \quad (3)$$

where \mathbf{R} is a 3 by 3 rotation matrix and \mathbf{t} is the translation vector. We can obtain \mathbf{R} and \mathbf{t} between two coordinates by calibration.

The human hand is joined by the interactive robot \mathcal{I} . Thus its position can be regarded as the same as the end-effector position of the interactive robot $\mathbf{x}_{\text{end-eff}}^I$. Using (3), we can track the human hand position in \mathcal{O}^D given \mathbf{R} and \mathbf{t} :

$$\mathbf{p}_h^D = \mathbf{R}\mathbf{x}_{\text{end-eff}}^I + \mathbf{t}. \quad (4)$$

Assuming the initial arm posture in \mathcal{O}^D is known and the shoulder does not move during the dressing, we can move the origin of \mathcal{O}^D to the shoulder by translation, we denote this frame as shoulder frame. From now on, for simplicity, unless explicitly denoted with superscript $^I \mathcal{D}$, all positions are with regard to the shoulder frame with its origin at the shoulder.

Since the shoulder is assumed static during dressing, the posture estimation problem boils down to recovering the elbow position \mathbf{p}_e given the hand position \mathbf{p}_h . A schematic diagram is shown in Fig. 5.

The human arm has seven degrees of freedom. Only four out of seven contribute to the displacement of the hand \mathbf{p}_h [43]. The four joint angles $\mathbf{q} = [\alpha \ \beta \ \phi \ \gamma]^T$ are depicted in Fig. 6. A spherical joint located at the shoulder with two degrees of freedom (α, β), and another spherical joint at the elbow with two degrees of freedom (ϕ, γ). The shoulder, elbow, and hand representation in the shoulder frame can be transformed into the angle representation and vice versa (given forearm and upper arm lengths). The hand position can be expressed as:

$$\mathbf{p}_h = \mathbf{f}(\mathbf{q}) \quad (5)$$

The hand movement:

$$\mathbf{p}_h + \Delta\mathbf{p}_h = \mathbf{f}(\mathbf{q} + \Delta\mathbf{q}) = \mathbf{f}(\mathbf{q}) + \mathbf{J}(\mathbf{q})\Delta\mathbf{q} + \text{h.o.t.}, \quad (6)$$

where

$$\mathbf{J}(\mathbf{q}) = \frac{\partial \mathbf{f}}{\partial \mathbf{q}}(\mathbf{q}) \in \mathbb{R}^{3 \times 4} \quad (7)$$

This then leads to:

$$\Delta\mathbf{p}_h = \mathbf{J}(\mathbf{q})\Delta\mathbf{q}. \quad (8)$$

For a given $\Delta\mathbf{p}_h$, (8) has infinite solutions of $\Delta\mathbf{q}$. We aim to find the $\Delta\mathbf{q}$ from (8) with good accuracy as compared to the human movement while enabling fast computation to be implemented in real-time. Thus, we define a quadratic optimization with an analytical solution:

$$\begin{aligned} \min_{\Delta\mathbf{q}} \mathbf{L} &= \Delta\mathbf{q}^T \mathbf{Q} \Delta\mathbf{q} \\ \text{s.t. } \Delta\mathbf{p}_h &= \mathbf{J}(\mathbf{q})\Delta\mathbf{q}, \end{aligned} \quad (9)$$

where \mathbf{Q} is a diagonal weighting matrix with non-zero diagonal elements for solving the optimal $\Delta\mathbf{q}$. Physically, \mathbf{Q} indicates how the hand velocity is distributed on each joint, a larger element on the diagonal indicates the corresponding joint is less likely to move during arm movements. We find \mathbf{Q} using the arm movement data recorded during the stretch and the detail is presented in Sect. VI-B.

The solution to the optimization problem (9) is (detailed derivation in the Appendix):

$$\Delta\mathbf{q}^* = \mathbf{J}^+ \Delta\mathbf{p}_h - (\boldsymbol{\mu}^T \mathbf{Q} \Delta\mathbf{q}_h / \boldsymbol{\mu}^T \mathbf{Q} \boldsymbol{\mu}) \boldsymbol{\mu},$$

where \mathbf{J}^+ is Moore–Penrose inverse of the \mathbf{J} and $\boldsymbol{\mu}$ is the null space vector of \mathbf{J}^3 . Current postures in angle representation are then:

$$\hat{\mathbf{q}}_T = \hat{\mathbf{q}}_{T-1} + \Delta\mathbf{q}^*. \quad (10)$$

³Detail solution can be found in the appendix

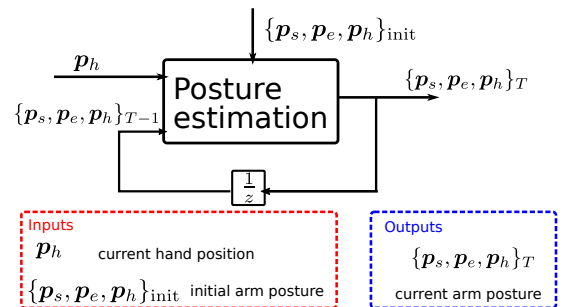


Fig. 5. A schematic diagram showing the inputs and outputs of the human posture estimation.

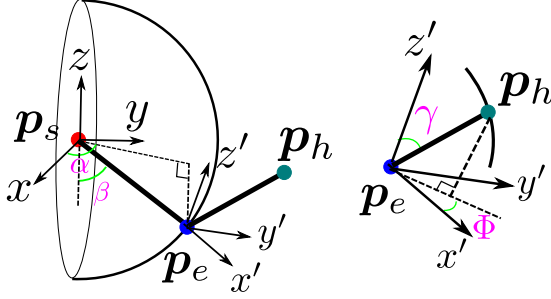


Fig. 6. Schematic representation of human arm from the shoulder to the hand with four joint angles. A spherical joint located at the shoulder with two degrees of freedom (α, β), and another spherical joint at the elbow with two degrees of freedom (ϕ, γ).

Note that this is a recursive estimation as depicted in Fig. 5. Only the initial value of \mathbf{q} is known such that $\dot{\mathbf{q}}_0 = \mathbf{q}_0$. The analytical solution can be computed fast online which allows us to use the estimation scheme in real-time during dressing.

Lastly, the angle representation $\dot{\mathbf{q}}_T$ is transformed into current positions of the shoulder, elbow, and hand $\{\hat{\mathbf{p}}_s, \hat{\mathbf{p}}_e, \hat{\mathbf{p}}_h\}_T$ for deriving the dressing policy. We evaluate the accuracy of the estimation scheme in Sect. VI-B.

V. DRESSING ROBOT – DRESSING COORDINATE-BASED LEARNING

The dressing is highly dependent on the human arm posture. Previous research explored such dependency in learning the dressing policy. In [44], the authors placed in simulation haptic sensor on each segment of the arm as observation in deep reinforcement learning. Others define task parameters as local coordinates at the shoulder, elbow, and hand and then encode the dressing policy with TP-GMM [6]–[8]. Similarly, we explore such dependencies and define an arm-posture-dependent coordinate system for encoding the dressing policy with LfD. In the following subsections, we first present the dressing coordinate then the LfD in the new coordinate system.

A. Dressing coordinate

The dressing motion follows the arm from the hand to the elbow and finally reaches the shoulder. The monotonic motion naturally leads us to introduce a scalar quantity to model the dressing progress. We denote the progress scalar as s .

The dressing motion is additionally constrained by the size of the armscye. Thus we use a polar coordinate around the forearm and the upper-arm for encoding the constraint: l , the distance to the arm, and θ , the angle around the arm. The formulation yields two cylinder coordinates on the forearm and the upper-arm. However, the complexity arises from the elbow where we require a smooth transition from the forearm coordinate to the upper arm coordinate (see Fig. 7a).

To enable the smooth transition, we use a part of a horn torus (A torus where the distance from the center of the tube to the center of the torus equals the radius of the tube) for connecting the two cylinder coordinate. As a result of the torus define around the elbow, the progress curve is divided into three pieces: a forearm segment, an elbow arc for a smooth

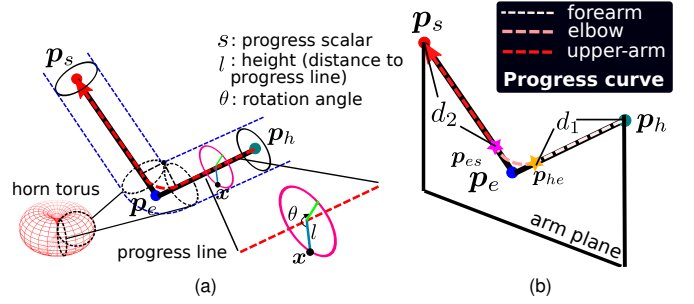


Fig. 7. The dressing coordinate is a cylinder coordinate defined around the arm, with a smoothing transitional corner around the elbow. The sub-figure (a) presents the full definition of the coordinate and (b) shows the progress curve in three segments.

transition to the upper arm, and an upper-arm segment as shown in Fig. 7b.

To convert a point on the dressing path $\mathbf{x} \in \mathbb{R}^3$ in Cartesian coordinate into the dressing coordinate $[s, l, \theta]$, we first project \mathbf{x} onto the arm plane given by the shoulder p_s , elbow p_e and hand positions p_h :

$$\mathbf{x}_{\text{arm}} = \mathbf{x} + \frac{\mathbf{v}(\mathbf{p}_h \cdot \mathbf{v} - \mathbf{x} \cdot \mathbf{v})}{|\mathbf{v}|^2}, \quad (11)$$

where \mathbf{v} is the vector perpendicular to the arm plane.

We further find the progress scalar of \mathbf{x}_{arm} on the progress curve. The progress curve is divided into 3 segments by 2 transitional points: p_{he} (transition from the forearm to elbow) and p_{es} (transition from elbow to upper arm) as shown by stars on Fig. 7b. The distance from p_h to p_{he} is denoted $|d_1|$, and from p_s to p_{es} is $|d_2|$.

We need to determine which segments \mathbf{x}_{arm} belongs to. To do that, we compute the distance \mathbf{x}_{arm} project onto the line defined by the forearm and upper-arm segments respectively:

$$\begin{aligned} d_{\text{forearm}} &= \frac{(\mathbf{x}_{\text{arm}} - \mathbf{p}_h) \cdot (\mathbf{p}_e - \mathbf{p}_h)}{|(\mathbf{p}_e - \mathbf{p}_h)|} \\ d_{\text{upperarm}} &= \frac{(\mathbf{x}_{\text{arm}} - \mathbf{p}_s) \cdot (\mathbf{p}_e - \mathbf{p}_s)}{|(\mathbf{p}_e - \mathbf{p}_s)|} \end{aligned} \quad (12)$$

The value of d_{forearm} and d_{upperarm} is then compared against d_1 and d_2 so that:

$$\mathbf{x}_{\text{arm}} \text{ on the } \begin{cases} \text{forearm} & \text{if } d_{\text{forearm}} < |d_1| \text{ and } d_{\text{upperarm}} > |d_2| \\ \text{upperarm} & \text{if } d_{\text{upperarm}} < |d_2| \text{ and } d_{\text{forearm}} > |d_1| \\ \text{elbow} & \text{otherwise} \end{cases}$$

Depending on which segment \mathbf{x}_{arm} belongs to, we find the corresponding $\mathbf{x}_{\text{curve}}$ (pink triangles on Fig. 8) on the progress curve for \mathbf{x}_{arm} . For the forearm and upper arm segment, calculating $\mathbf{x}_{\text{curve}}$ is straightforward. For the elbow segment, we find the line connecting the center of the elbow arc to \mathbf{x}_{arm} . The intersection point between the line and the progress curve is $\mathbf{x}_{\text{curve}}$ (See Fig. 8).

We then define $s = 0$ for $\mathbf{x}_{\text{curve}} = \mathbf{p}_h$, $s = 1$ for $\mathbf{x}_{\text{curve}} = \mathbf{p}_s$, for any $\mathbf{x}_{\text{curve}}$, we have:

$$s = \begin{cases} \frac{d_{\text{forearm}}}{|d_{\text{curve}}|} & \text{if } \mathbf{x}_{\text{curve}} \text{ is on the forearm} \\ \frac{|d_{\text{curve}}| - d_{\text{upperarm}}}{|d_{\text{curve}}|} & \text{if } \mathbf{x}_{\text{curve}} \text{ is on the upperarm} \\ \frac{d_1 + \omega r}{|d_{\text{curve}}|} & \text{if } \mathbf{x}_{\text{curve}} \text{ is on the upperarm} \end{cases}$$

where $|d_{\text{curve}}|$ is the full length of the progress curve from p_h to p_s , ω is the angle of x_{curve} on the elbow arc and r is the radius of the elbow segment on the progress curve.

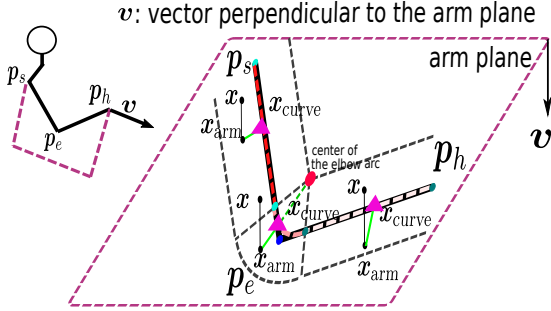


Fig. 8. Graphic illustration of finding the corresponding point on the progress curve x_{curve} given a random point x on the dressing path in Cartesian coordinate. The point x is first projected onto the arm plane to get x_{arm} . Then we determine which segment x_{arm} belongs to on the progress curve. Finally we find the corresponding x_{curve} .

Once we found the projection of the dressing position on the progress curve x_{curve} and the progress scalar s , we can calculate the distance to the arm l and the angle around the arm θ as follows.

The length l of x is:

$$l = |x - x_{\text{curve}}| \quad (13)$$

We define v as the reference 0° for the angle θ computation. The θ is defined as

$$\theta = \angle(x_{\text{curve}} - x, v) \quad (14)$$

Note that v has two directions, one pointing towards to the human body and the other pointing outwards. We select the former to avoid flipping angles from 0 to 2π during the dressing motion.

By converting the Cartesian coordinate to the dressing coordinate and obtaining the motion generation model in the dressing coordinate, we can:

- limit the policy space to be around the arm by imposing the maximum value for the length l ,
- ensure the motion convergence to the vicinity of the shoulder by progress scalar s ,
- transfer the trained motion generation model on one arm to another as the data is relative to the arm posture.

Note one prerequisite for the last statement is that the ratio between the forearm and upper arm is similar among people.

B. LfD in dressing coordinate

For LfD in dressing coordinate, we employ Gaussian Mixture Models (GMM) and Gaussian Mixture Regression (GMR) for learning and generating the dressing policy [45]. The GMM/GMR-based imitation learning offers fast movement retrieval and versatile inputs/outputs arrangement which is desirable for our task. Please note that the LfD algorithm is not a part of our contribution and it is possible to use different methods/formulations for learning the policy in the dressing coordinate.

We first briefly describe GMM/GMR-based LfD then show how to apply it to learning the dressing policy.

GMM models the joint distribution of the demonstration data. We denote the demonstrated data ξ :

$$\xi = [\xi^{\mathcal{I}}, \xi^{\mathcal{O}}]^T. \quad (15)$$

with $\xi^{\mathcal{I}}$ is the input and $\xi^{\mathcal{O}}$ the output. The probability density function $p(\xi_i)$ is estimated with K Gaussian distributions:

$$p(\xi_i) = \sum_{k=1}^K \pi_k \mathcal{N}(\xi_i | \mu_k, \Sigma_k)$$

where μ_k and Σ_k are mean and variance of the k th Gaussian. To determine an optimal number of Gaussian K for GMM, we make use of the Bayesian Information Criterion (BIC) [46] for balancing the model complexity and representation quality.

Once K is selected, we can initialize the GMM with K-Means clustering and then employ the Expectation-Maximization algorithm to iteratively compute the model parameters $\{\pi_k, \mu_k, \Sigma_k\}_{k=1}^K$.

The resulting K Gaussian parameters can be decomposed as:

$$\mu_k = \begin{bmatrix} \mu_k^{\mathcal{I}} \\ \mu_k^{\mathcal{O}} \end{bmatrix}, \quad \Sigma_k = \begin{bmatrix} \Sigma_k^{\mathcal{I}} & \hat{\Sigma}_k^{\mathcal{I}\mathcal{O}} \\ \Sigma_k^{\mathcal{O}\mathcal{I}} & \hat{\Sigma}_k^{\mathcal{O}} \end{bmatrix}. \quad (16)$$

Given input data the output is retrieved using GMR by conditioning on the input data [47].

For encoding dressing with GMM/GMR in the dressing coordinate, we demonstrate the dressing task with static arm postures, the arm posture, and the dressing path is recorded for converting the dressing path into the dressing coordinate. We use the progress scalar s and the elbow angle ϕ as inputs. The outputs are the differences in the distance to the arm δl , and the angle difference around the arm $\delta \theta$. The differences are computed with regard to the starting position in the demonstration. For all demonstrations, we start from above the hand of the human.

VI. EXPERIMENTS

We conduct 3 different experiments to investigate various aspects of the proposed framework.

In Sect. VI-A, we investigate the effect of the elbow angle on the dressing strategy using expert demonstration data of static arm postures with different elbow angles. Then in Sect. VI-B we evaluate the arm posture estimation scheme to show that it is accurate enough for the dressing task.

Lastly, in Sect. VI-C we showcase our interactive dressing framework with real robot experiments. To demonstrate the flexibility of the defined dressing coordinate, we train the policy from demonstrations on a mannequin and apply the policy to a human arm. We conduct an ablation study where we disable the stretch movement and dress with a static human arm. Furthermore, we test the framework under cases where the human is not fully compliant with the interactive robot and show that the overall framework still works well. In these experiments, the robot dresses the human in short and long sleeves shirts with different materials. Note that the automatic dressing of long sleeves shirts are unprecedented in previous research.

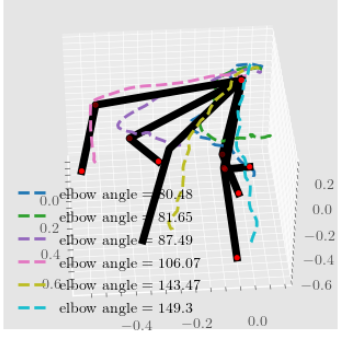


Fig. 9. Static arm postures with different elbow angles and the corresponding expert demonstrations of dressing with these postures.

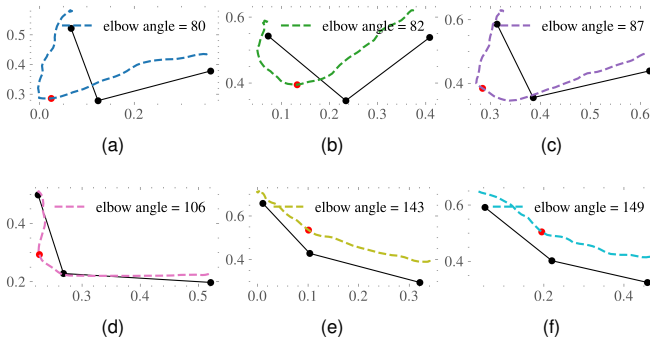


Fig. 10. The projection of the arm postures and the corresponding demonstrated dressing path on the arm plane. The red dot is a transition point corresponding to the middle of the elbow arc on the progress curve.

A. Effect of the elbow angle on dressing strategies

In Sect. IV-A we discussed the effect of the elbow angle on the dressing strategy with diminished rigidity. In this section, we aim to show this effect with expert demonstration data.

We collect demonstration data through kinesthetic teaching with a Franka robot under different arm postures. The dressing paths and arm postures are recorded in the process. To validate whether the elbow angle affects the dressing strategies, we project the path onto the arm plane. In Fig. 9 we present 6 postures with different elbow angles and the corresponding dressing path on the arm plane.

The projection of the arm postures (in black solid line) and the corresponding demonstrated dressing path (colored dash line) on the arm plane are shown in Fig. 10. The red dot is a transition point corresponding to the middle of the elbow arc in Fig. 7b on the progress curve.

In addition, we provide a quantitative result summarized in Tab. I. We calculate the distance between the transition point and the elbow. When the transition point is on the inner arm plane, the distance is positive which indicates that the dressing employs an inner strategy. When the transition point is on the outer arm plane, we set the distance negative which indicates that the dressing employs an outer strategy (see Sect. IV-B and Fig. 3 for the definition of inner/outer strategy).

We can observe both from Fig. 10 and Tab. I that the outer dressing strategy is employed when the elbow angle is small, which justifies our analysis in Sect. IV-A.

TABLE I
ELBOW ANGLE AND CORRESPONDING DISTANCE BETWEEN THE TRANSITION POINT AND THE ELBOW ON THE ARM PLANE.

elbow angle (°)	80.47	81.65	87.49	106.07	143.46	149.30
distance (m)	-0.099	-0.11	-0.10	-0.07	0.107	0.105

B. Evaluation of the posture estimation scheme

As the dressing path is highly dependent on the arm posture, posture estimation is crucial to the success of dressing. In this section, we provide a quantitative evaluation of the posture estimation scheme. We consider

- 1) the shoulder is static during dressing which is a common assumption in assistive dressing literature [6], [10],
- 2) the initial arm posture (in the dressing robot frame \mathcal{O}^D) is known.

With the above assumptions and real-time hand position recovery from the interactive robot (see. Sect. IV-C), the only estimated quantity in the full posture description $\mathbf{P} = \{\mathbf{p}_s, \mathbf{p}_e, \mathbf{p}_h\}$ is the elbow position \mathbf{p}_e .

Thus in the evaluation, for a series of arm postures during movements $\{\mathbf{P}_0, \mathbf{P}_1, \dots, \mathbf{P}_T\}$, we use the maximum error of the elbow as the performance indicator of our posture estimation scheme:

$$\text{error}_{\max} = \max_{i=1}^T |\mathbf{p}_e(i) - \hat{\mathbf{p}}_e(i)|$$

where $\hat{\mathbf{p}}_e(i)$ is the estimated elbow position at the i^{th} instance.

One tuneable parameter that affects the estimation performance is the diagonal weight matrix D in (9). We compute D using the movement data $\{\mathbf{P}_0, \mathbf{P}_1, \dots, \mathbf{P}_T\}$. The data is first transformed to angle representation $\{\mathbf{q}_0, \mathbf{q}_1, \dots, \mathbf{q}_T\}$ (refer to Sect. IV-C and Fig. 5 for the definition of angle representation and 4 angles $\mathbf{q} = [\alpha \ \beta \ \phi \ \gamma]^T$ associated). We then compute the difference between adjacent angles and yield:

$$\{\delta \mathbf{q}_1, \delta \mathbf{q}_2, \dots, \delta \mathbf{q}_T\}, \quad (17)$$

where

$$\delta \mathbf{q}_i = [\delta \alpha_i \ \delta \beta_i \ \delta \phi_i \ \delta \gamma_i]^T = \mathbf{q}_i - \mathbf{q}_{i-1}. \quad (18)$$

The weighting diagonal matrix \mathbf{Q} in (9) is calculated as:

$$\mathbf{Q} = \text{diag}\left\{\frac{1}{\sum_{i=1}^T \delta \alpha_i^2}, \frac{1}{\sum_{i=1}^T \delta \beta^2}, \frac{1}{\sum_{i=1}^T \delta \phi_i^2}, \frac{1}{\sum_{i=1}^T \delta \gamma_i^2}\right\}$$

For the evaluation, we conduct experiments to collect arm movement data with an XSens motion capture suit. During the data collection phase, one person is asked to stretch the arm of the other. The posture data was collected using the suit and regarded as ground truth. We then compared the estimated elbow position with the ground truth. We collected 4 movement patterns from different starting poses. The maximum error during the stretch motion is presented in Tab. II.

TABLE II
THE MAXIMUM ERROR IN ELBOW ESTIMATION DURING THE STRETCH.

case number	1	2	3	4
error _{max} (m)	0.028	0.026	0.032	0.028

Figure 11 shows the ground truth and the estimated elbow position (x, y, z) in solid and dash line respectively in all 4 cases.

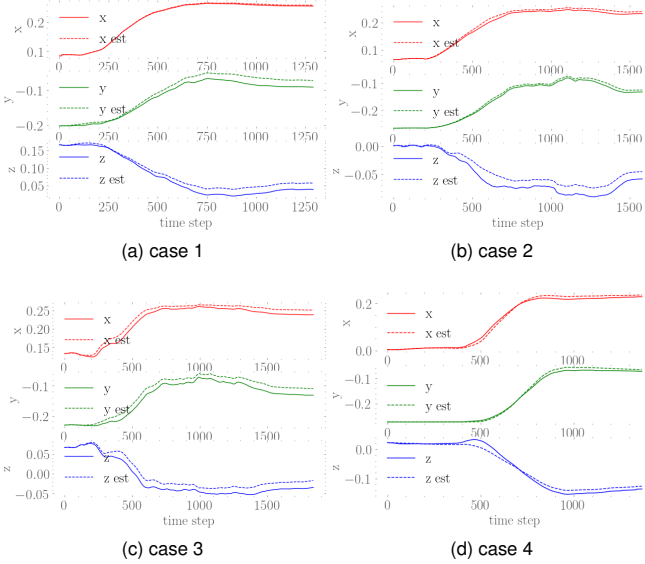


Fig. 11. The ground truth and the estimated elbow position (x, y, z) in solid and dash line respectively in test cases.

We observe that generally, the deviation from ground truth is larger as the time step increases, this is probably due to the recursive nature of the estimation scheme. The error may accumulate with time. Despite this, the maximum error is around 3 centimeters which is much smaller than the size of the armscye. It is compatible with the results from [11] which proposed a vision-based estimation of the elbow position during dressing under occlusion.

C. Interactive dressing

In this section, we show the experimental results of our interactive dressing scheme. We present experiments with three types of clothes: a short and rigid sleeve shirt, a long and rigid sleeve shirt, and a long and soft sleeve shirt.

To show the flexibility of our framework, our demonstrations were collected on the mannequin and the learned dressing policy was executed on the human arm. In demonstrations, we always start around above the hand and with the same orientation⁴. The arm length of both the human and the mannequin is listed in Tab. III, although having different lengths, the ratio between hand-elbow and elbow-shoulder is similar. Since we encode the data in the dressing coordinate which is independent of the arm lengths, thus enables direct transfer of the dressing policy.

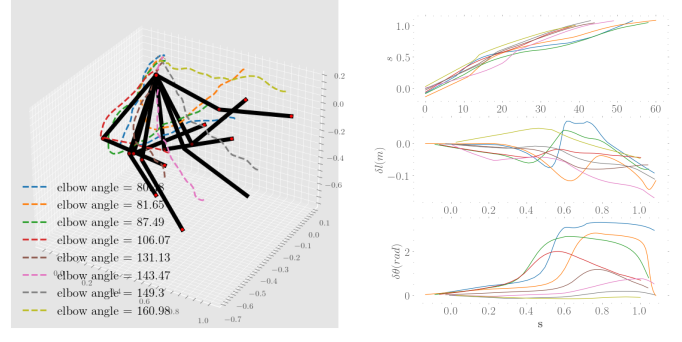
Fig. 12 shows the demonstration and transformed data in the dressing coordinate. For the angle around the arm θ and the distance to the arm l , we present the changes during dressing $\delta\theta$ and δl instead of the absolute values. The difference is computed with regard to the starting position which is around above the hand. For postures with smaller elbow angles, we

⁴The orientation can be seen in the start configuration in dressing in Fig. 14

TABLE III
ARM LENGTHS OF THE HUMAN AND THE MANNEQUIN

	hand - elbow (cm)	elbow - shoulder (cm)	ratio
mannequin	26	25	1.04
human	30	29	1.03

can observe a change in the angles around the arm θ since it needs to move to the back of the arm to execute an outer strategy.



(a) Expert demonstrations on different postures (b) Demonstrations transformed into the dressing coordinates

Fig. 12. The expert demonstrations on different postures used for training dressing policy and the transformed data in the dressing coordinate.

From Fig. 12b we observe that the progress scalar s is a monotonic increasing quantity. Consider a target s_{target} , we model s with a dynamical system with a constant increment $c > 0$:

$$s_{T+1} = s_T + \min(c, (s_{\text{target}} - s_T)) \quad (19)$$

We respectively trained two GMM for the changes in angles around the arm $\delta\theta$ and changes in the distance to the arm δl with inputs progress scalar s and the elbow angle ϕ ⁵. We use 8 Gaussians for both δl and $\delta\theta$. The resulting mixture models are presented in 3D surf plots in Fig. 13. We can observe a smaller elbow angle displays larger changes in θ which is a clear indication for taking the outer strategy. For a large elbow angle, the θ change is almost zero which resembles an inner strategy. Due to the diminishing rigidity, the end effector rotation has a very limited effect during dressing. In the experiment, we consider only the z axis orientation of the end-effector of the dressing robot. The z axis rotation is applied to avoid collision with the arm during dressing. We can use a constant incremental rotation with regard to s or a separate GMM with the same inputs (s, ϕ) for encoding the difference dz in z axis rotation (The training procedure is the same as $\delta\theta$ and δl).

We implement the policy with our optimal stretch and also posture estimation scheme. Three types of experiments are conducted:

- 1) Human passively follows the interactive robot
- 2) Human is not fully compliant with the guiding force and moves in other directions
- 3) Ablation study: human arm remains static

⁵Please note that other formulations may be also possible, such as to learn the joint distribution of $[s, \phi, l, \theta]$

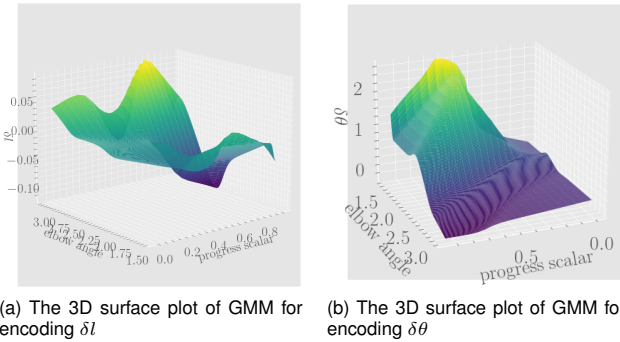


Fig. 13. The surface plot for GMM with elbow angles ψ and progress scalar s as inputs and outputs changes in the distance to the arm δ_l and changes in angles around the arm $\delta\theta$ respectively.

We tested in different starting postures and different clothes as shown in Fig. 14. In the figure, we present only starting and end configurations, the full dressing sequences are recorded in the video accompanying the paper. We tested the dressing while the human passively follows the guiding force and also moves in other directions (not fully compliant). When the human is not fully compliant, in the figure, we also display with high transparency a nominal end configuration when the human is compliant. The deviation from the nominal end configuration is indicated by a blue arrow. With these results, we prove that humans can move in other directions if desired and the framework is robust against non-compliant behavior and still succeed in dressing.

In the ablation study, we demonstrate cases where the elbow angle is small, and the cloth tends to get stuck around the elbow, thus reiterating the importance of having a bimanual setup for dressing. However, the result also suggests that if the human starts in these postures and refuses to move along with the guiding force, the dressing could fail.

VII. CONCLUSION

Traditional assistive dressing considers a *one-robot-to-one-arm* setup, which

- either assumes static arm posture or requires additional sensors and algorithms for tracking the arm posture,
- renders the human arm hanging in the air during the dressing process which is often tiring,
- may fail/get stuck at the elbow for some initial arm postures.

In the light of the following limitations, and inspired by strategies taken by caregiving experts, we designed a bimanual assistive dressing framework with a *two-robot-to-one-arm* setup that

- allows tracking of arm postures without additional sensors,
- provides support and guiding force for the arm being dressed,
- stretches the human arm while compliant to obtain postures for the ease of dressing.

We approached the design by first analysing the effect of elbow angle in dressing. Based on this effect, we proposed

an optimal stretch controller for the interactive robot. As the interactive robot holds the human hand, the arm posture can be estimated in real-time with inverse kinematics. For the dressing robot, we utilize the dependency of the dressing policy on the arm posture and introduced a dressing coordinate defined by the arm posture for easy encoding of the dressing policy from demonstrations.

The adoption of the dressing coordinate greatly enhances the flexibility of the LfD. The trained policy can adapt to different arm lengths as long as the forearm to upper-arm ratio is similar. The framework allows dressing different types of clothes, even long sleeves which is unprecedented in previous research. The dressing remains robust even though human is not fully compliant with the guidance from the interactive robot.

Since this is the first time such a bimanual setup was employed in dressing a human, there are two major limitations of the proposed framework:

- The assumption of the shoulder remains static is not always true, since the interactive robot is stretching the arm, the shoulder is more likely to move forward. A forward-moving shoulder will subsequently increase the length of the arm (as now the hand can reach further when fully stretched). The increased length may render the arm posture estimation scheme unsolvable thus the overall scheme will fail.
- The elbow angle is identified as the crucial parameter that affects dressing, however, there is no explicit coordination between the dressing and interactive robot to make sure that when the dressing robot is going through the elbow, the interactive robot already makes the elbow angle sufficiently large to avoid getting stuck.

It is difficult to solve the first limitation purely from the algorithm side, one possibility is to combine inverse kinematics with vision-based tracking for more accurate posture estimation. The second limitation is even trickier, to make the coordination explicit, a thorough analysis of dressing on different elbow angles needs to be conducted to determine a boundary condition of the elbow angle, then additionally, an assumption has to be placed on the human side (passive for instance) to make sure that the interactive robot will always succeed in bringing the human arm into favorable postures before dressing arm reach the elbow.

Another possible direction for future work is safety analysis. We did not explicitly analyze the safety of the overall system. However, for assistive robots, it is crucial to ensure human safety during robotic assistance. Inspirations for conducting system-level safety analysis can be drawn from [48].

Despite the above-mentioned limitations, our proposal is the first that considers interactive dressing assistance with a bimanual setup. The setup is inspired by caregiving experts conducting the task, which makes the scheme receptive to humans. It represents a paradigm shift in thinking of the dressing task from a *one-robot-to-one-arm* setup to a *two-robot-to-one-arm* setup.



Fig. 14. Starting and/or end configurations for 3 different experiments: human passive/compliant, human not fully compliant, and the ablation study where the human remains static. For experiments where the human is not fully compliant, we also display with high transparency a nominal end configuration when the human is compliant. The deviation from the nominal end configuration is indicated by a blue arrow.

ACKNOWLEDGMENTS

This work was supported by Honda Research Institute Europe GmbH as part of the project: Learning Physical Human-Robot Cooperation Tasks.

APPENDIX

In the Appendix, we provide the analytical solution to (9) in Sect. IV-C:

$$\begin{aligned} \min_{\Delta q} \mathbf{L} &= \Delta q^T \mathbf{Q} \Delta q \\ \text{s.t. } \Delta p_h &= \mathbf{J} \Delta q \end{aligned}$$

Since $\mathbf{J} \in \mathbb{R}^{3 \times 4}$, $\Delta p_h = \mathbf{J} \Delta q$ has infinite number of solutions:

$$\Delta q = \mathbf{J}^+ \Delta p_h + \lambda \boldsymbol{\mu} = \Delta q_h + \lambda \boldsymbol{\mu} \quad (20)$$

where \mathbf{J}^+ is the Moore-Penrose inverse of the \mathbf{J} and $\boldsymbol{\mu}$ is the vector in the null space of \mathbf{J} (e.g., $\mathbf{J} \boldsymbol{\mu} = \mathbf{0}$), and $\lambda \in \mathbb{R}$ is a gain. Taking (21) into \mathbf{L} :

$$\begin{aligned} \mathbf{L} &= (\Delta q_h + \lambda \boldsymbol{\mu})^T \mathbf{Q} (\Delta q_h + \lambda \boldsymbol{\mu}) \\ &= (\boldsymbol{\mu}^T \mathbf{Q} \boldsymbol{\mu}) \lambda^2 + 2 \boldsymbol{\mu}^T \mathbf{Q} \Delta q_h \lambda + \Delta q_h^T \mathbf{Q} \Delta q_h \end{aligned} \quad (21)$$

which is quadratic in λ .

The original optimization problem can be transformed into:

$$\min_{\lambda} \mathbf{L} = (\boldsymbol{\mu}^T \mathbf{Q} \boldsymbol{\mu}) \lambda^2 + 2 \boldsymbol{\mu}^T \mathbf{Q} \Delta q_h \lambda + \Delta q_h^T \mathbf{Q} \Delta q_h \quad (22)$$

Let us denote $\boldsymbol{\mu}^T \mathbf{Q} \boldsymbol{\mu} = a$, $\boldsymbol{\mu}^T \mathbf{Q} \Delta q_h = b$ and $\Delta q_h^T \mathbf{Q} \Delta q_h = c$:

$$\begin{aligned} \mathbf{L} &= a \lambda^2 + 2b \lambda + c \\ &= a(\lambda^2 + 2 \frac{b}{a} \lambda + c) \\ &= a((\lambda + \frac{b}{a})^2 + c - \frac{b^2}{a^2}) \end{aligned} \quad (23)$$

The solution that minimize \mathbf{L} is:

$$\lambda = -\frac{b}{a} = -\boldsymbol{\mu}^T \mathbf{Q} \Delta q_h / \boldsymbol{\mu}^T \mathbf{Q} \boldsymbol{\mu} \quad (24)$$

Taking (24) into (21) we can obtain the optimal solution:

$$\Delta q^* = \mathbf{J}^+ \Delta p_h - (\boldsymbol{\mu}^T \mathbf{Q} \Delta q_h / \boldsymbol{\mu}^T \mathbf{Q} \boldsymbol{\mu}) \boldsymbol{\mu} \quad (25)$$

The first term ensures that the constraint is respected; on the other hand, the second term generates a null-space transition that minimizes the total weighted joint displacement.

REFERENCES

- [1] “Ageing and health,” Oct 2021. [Online]. Available: <https://www.who.int/news-room/fact-sheets/detail/ageing-and-health>
- [2] B. J. Dudgeon, J. M. Hoffman, M. A. Ciol, A. Shumway-Cook, K. M. Yorkston, and L. Chan, “Managing activity difficulties at home: a survey of medicare beneficiaries,” *Archives of physical medicine and rehabilitation*, vol. 89, no. 7, pp. 1256–1261, 2008.
- [3] D. J. Agrawale, A. Cherubini, A. Sherikov, P.-B. Wieber, and A. Kheddar, “Human-humanoid collaborative carrying,” *IEEE Transactions on Robotics*, vol. 35, no. 4, pp. 833–846, 2019.
- [4] S. Tarbouriech, B. Navarro, P. Fraisse, A. Crosnier, A. Cherubini, and D. Sallé, “Admittance control for collaborative dual-arm manipulation,” in *2019 IEEE Int. Conf. on Advanced Robotics*. IEEE, 2019.
- [5] L. van der Spaa, M. Gienger, T. Bates, and J. Kober, “Predicting and optimizing ergonomics in physical human-robot cooperation tasks,” in *2020 IEEE International Conference on Robotics and Automation (ICRA)*. IEEE, 2020, pp. 1799–1805.
- [6] E. Pignat and S. Calinon, “Learning adaptive dressing assistance from human demonstration,” *Robotics and Autonomous Systems*, vol. 93, pp. 61–75, 2017.
- [7] J. Hoyos, F. Prieto, G. Alenyà, and C. Torras, “Incremental learning of skills in a task-parameterized Gaussian mixture model,” *Journal of Intelligent & Robotic Systems*, vol. 82, no. 1, pp. 81–99, 2016.
- [8] J. Zhu, M. Gienger, and J. Kober, “Learning task-parameterized skills from few demonstrations,” *IEEE Robotics and Automation Letters*, vol. 7, no. 2, pp. 4063–4070, 2022.

[9] Y. Gao, H. J. Chang, and Y. Demiris, “User modelling for personalised dressing assistance by humanoid robots,” in *2015 IEEE/RSJ Int. Conf. on Intelligent Robots and Systems*. IEEE, 2015, pp. 1840–1845.

[10] F. Zhang, A. Cully, and Y. Demiris, “Probabilistic real-time user posture tracking for personalized robot-assisted dressing,” *IEEE Transactions on Robotics*, vol. 35, no. 4, pp. 873–888, 2019.

[11] G. Chance, A. Jevtić, P. Caleb-Solly, G. Alenyà, C. Torras, and S. Dogramadzi, ““elbows out”—predictive tracking of partially occluded pose for robot-assisted dressing,” *IEEE Robotics and Automation Letters*, vol. 3, no. 4, pp. 3598–3605, 2018.

[12] Z. Erickson, M. Collier, A. Kapusta, and C. C. Kemp, “Tracking human pose during robot-assisted dressing using single-axis capacitive proximity sensing,” *IEEE Robotics and Automation Letters*, vol. 3, no. 3, pp. 2245–2252, 2018.

[13] Y. Wang, D. Held, and Z. Erickson, “Visual haptic reasoning: Estimating contact forces by observing deformable object interactions,” *arXiv preprint arXiv:2208.05632*, 2022.

[14] T. Tamei, T. Matsubara, A. Rai, and T. Shibata, “Reinforcement learning of clothing assistance with a dual-arm robot,” in *2011 11th IEEE-RAS Int. Conf. on Humanoid Robots*. IEEE, 2011, pp. 733–738.

[15] K. Yamazaki, R. Oya, K. Nagahama, K. Okada, and M. Inaba, “Bottom dressing by a dual-arm robot using a clothing state estimation based on dynamic shape changes,” *International Journal of Advanced Robotic Systems*, vol. 13, no. 1, p. 5, 2016.

[16] G. Canal, E. Pignat, G. Alenyà, S. Calinon, and C. Torras, “Joining high-level symbolic planning with low-level motion primitives in adaptive hri: Application to dressing assistance,” in *2018 IEEE International Conference on Robotics and Automation (ICRA)*. IEEE, 2018, pp. 3273–3278.

[17] A. Jevtić, A. F. Valle, G. Alenyà, G. Chance, P. Caleb-Solly, S. Dogramadzi, and C. Torras, “Personalized robot assistant for support in dressing,” *IEEE transactions on cognitive and developmental systems*, vol. 11, no. 3, pp. 363–374, 2018.

[18] A. Kapusta, Z. Erickson, H. M. Clever, W. Yu, C. K. Liu, G. Turk, and C. C. Kemp, “Personalized collaborative plans for robot-assisted dressing via optimization and simulation,” *Autonomous Robots*, vol. 43, no. 8, pp. 2183–2207, 2019.

[19] A. Clegg, Z. Erickson, P. Grady, G. Turk, C. C. Kemp, and C. K. Liu, “Learning to collaborate from simulation for robot-assisted dressing,” *IEEE Robotics and Automation Letters*, vol. 5, no. 2, pp. 2746–2753, 2020.

[20] W. Yu, A. Kapusta, J. Tan, C. C. Kemp, G. Turk, and C. K. Liu, “Haptic simulation for robot-assisted dressing,” in *2017 IEEE international conference on robotics and automation (ICRA)*. IEEE, 2017, pp. 6044–6051.

[21] A. Kapusta, W. Yu, T. Bhattacharjee, C. K. Liu, G. Turk, and C. C. Kemp, “Data-driven haptic perception for robot-assisted dressing,” in *2016 25th IEEE international symposium on robot and human interactive communication (RO-MAN)*. IEEE, 2016, pp. 451–458.

[22] Z. Erickson, A. Clegg, W. Yu, G. Turk, C. K. Liu, and C. C. Kemp, “What does the person feel? learning to infer applied forces during robot-assisted dressing,” in *2017 IEEE International Conference on Robotics and Automation (ICRA)*. IEEE, 2017, pp. 6058–6065.

[23] L. Twardon and H. Ritter, “Active boundary component models for robotic dressing assistance,” in *2016 IEEE/RSJ Int. Conf. on Intelligent Robots and Systems (IROS)*. IEEE, 2016, pp. 2811–2818.

[24] S. Li, N. Figueira, A. J. Shah, and J. A. Shah, “Provably safe and efficient motion planning with uncertain human dynamics,” in *Robotics: Science and Systems*, 2021.

[25] S. Li, T. Stouraitis, M. Gienger, S. Vijayakumar, and J. A. Shah, “Set-based state estimation with probabilistic consistency guarantee under epistemic uncertainty,” *IEEE Robotics and Automation Letters*, vol. 7, no. 3, pp. 5958–5965, 2022.

[26] F. Zhang and Y. Demiris, “Learning grasping points for garment manipulation in robot-assisted dressing,” in *2020 IEEE International Conference on Robotics and Automation (ICRA)*. IEEE, 2020, pp. 9114–9120.

[27] M. Dragusanu, S. Marullo, M. Malvezzi, G. M. Achilli, M. C. Valigi, D. Prattichizzo, and G. Salvietti, “The dressgripper: A collaborative gripper with electromagnetic fingertips for dressing assistance,” *IEEE Robotics and Automation Letters*, vol. 7, no. 3, pp. 7479–7486, 2022.

[28] F. Krebs and T. Asfour, “A bimanual manipulation taxonomy,” *IEEE Robotics and Automation Letters*, 2022.

[29] L. P. Ureche and A. Billard, “Constraints extraction from asymmetrical bimanual tasks and their use in coordinated behavior,” *Robotics and autonomous systems*, vol. 103, pp. 222–235, 2018.

[30] A. Colomé and C. Torras, “Dimensionality reduction for dynamic movement primitives and application to bimanual manipulation of clothes,” *IEEE Transactions on Robotics*, vol. 34, no. 3, pp. 602–615, 2018.

[31] F. Suárez-Ruiz, X. Zhou, and Q.-C. Pham, “Can robots assemble an ikea chair?” *Science Robotics*, vol. 3, no. 17, p. eaat6385, 2018.

[32] J. Liu, Y. Chen, Z. Dong, S. Wang, S. Calinon, M. Li, and F. Chen, “Robot cooking with stir-fry: Bimanual non-prehensile manipulation of semi-fluid objects,” *IEEE Robotics and Automation Letters*, vol. 7, no. 2, pp. 5159–5166, 2022.

[33] J. Xu, G. G. Grindle, B. Salatin, J. J. Vazquez, H. Wang, D. Ding, and R. A. Cooper, “Enhanced bimanual manipulation assistance with the personal mobility and manipulation appliance (permma),” in *2010 IEEE/RSJ International Conference on Intelligent Robots and Systems*. IEEE, 2010, pp. 5042–5047.

[34] M. Connan, M. Sierotowicz, B. Henze, O. Porges, A. Albu-Schäffer, M. A. Roa, and C. Castellini, “Learning to teleoperate an upper-limb assistive humanoid robot for bimanual daily-living tasks,” *Biomedical Physics & Engineering Express*, vol. 8, no. 1, p. 015022, 2021.

[35] A. Edsinger and C. C. Kemp, “Two arms are better than one: A behavior based control system for assistive bimanual manipulation,” in *Recent progress in robotics: Viable robotic service to human*. Springer, 2007, pp. 345–355.

[36] A. Toshev and C. Szegedy, “Deeppose: Human pose estimation via deep neural networks,” in *Proceedings of the IEEE conference on computer vision and pattern recognition*, 2014, pp. 1653–1660.

[37] Z. Cao, T. Simon, S.-E. Wei, and Y. Sheikh, “Realtime multi-person 2d pose estimation using part affinity fields,” in *Proceedings of the IEEE conference on computer vision and pattern recognition*, 2017, pp. 7291–7299.

[38] R. A. Güler, N. Neverova, and I. Kokkinos, “Densepose: Dense human pose estimation in the wild,” in *Proceedings of the IEEE conference on computer vision and pattern recognition*, 2018, pp. 7297–7306.

[39] U. Iqbal, A. Doering, H. Yasin, B. Krüger, A. Weber, and J. Gall, “A dual-source approach for 3d human pose estimation from single images,” *Computer Vision and Image Understanding*, vol. 172, pp. 37–49, 2018.

[40] D. Berenson, “Manipulation of deformable objects without modeling and simulating deformation,” in *2013 IEEE/RSJ International Conference on Intelligent Robots and Systems*. IEEE, 2013, pp. 4525–4532.

[41] N. Hogan, “Impedance control: An approach to manipulation,” in *1984 American control conference*. IEEE, 1984, pp. 304–313.

[42] L. Sciavicco and B. Siciliano, *Modelling and control of robot manipulators*. Springer Science & Business Media, 2001.

[43] M. Desmurget and C. Prablanc, “Postural control of three-dimensional prehension movements,” *Journal of neurophysiology*, vol. 77, no. 1, pp. 452–464, 1997.

[44] A. Clegg, W. Yu, J. Tan, C. K. Liu, and G. Turk, “Learning to dress: Synthesizing human dressing motion via deep reinforcement learning,” *ACM Transactions on Graphics (TOG)*, vol. 37, no. 6, pp. 1–10, 2018.

[45] S. Calinon, F. Guenter, and A. Billard, “On learning, representing, and generalizing a task in a humanoid robot,” *IEEE Transactions on Systems, Man, and Cybernetics, Part B (Cybernetics)*, vol. 37, no. 2, pp. 286–298, 2007.

[46] G. Schwarz, “Estimating the dimension of a model,” *The annals of statistics*, 1978.

[47] M. Muhlig, M. Gienger, S. Hellbach, J. J. Steil, and C. Goerick, “Task-level imitation learning using variance-based movement optimization,” in *2009 IEEE International Conference on Robotics and Automation*. IEEE, 2009, pp. 1177–1184.

[48] J. A. McDermid, Y. Jia, and I. Habli, “Towards a framework for safety assurance of autonomous systems,” in *Artificial Intelligence Safety 2019*. CEUR Workshop Proceedings, 2019, pp. 1–7.